Laser-rf double-resonance measurements of the hyperfine structure in Sc II

N. B. Mansour, T. Dinneen,* and L. Young
Physics Division, Argonne National Laboratory, Argonne, Illinois 60439

K. T. Cheng
Lawrence Livermore National Laboratory, Livermore, California 94450
(Received 26 August 1988; revised manuscript received 13 February 1989)

The hyperfine structure of all levels of the metastable $3d^2$ configuration in Sc II has been measured with high precision by collinear fast-ion laser-rf double-resonance spectroscopy. The double-resonance technique improved the precision of the earlier results by more than a factor of 150. The enhanced precision made possible for the first time a meaningful comparison between experimental and multiconfiguration Dirac-Fock calculated B values. The comparison showed that, unlike the A values where disagreements between experiment and theory could be greater than 400%, the B values were well predicted.

I. INTRODUCTION

The laser-rf double-resonance technique introduced by Rosner *et al.*,[1] has proven to be a valuable method for high-precision spectroscopy. In the past, most of the information on the structure of ions has been provided from the optical spectra of discharge sources. Lately, there has been significant progress in the application of rf spectroscopic techniques to ions.[2] High-precision rf experiments on ions have been performed in ion-storage traps,[3,4] discharge cells, and on ion beams.[5–7] The laser-rf double-resonance technique, used in this work, is similar to atomic-beam magnetic resonance[8] with the fundamental difference being the replacement of large inhomogeneous magnetic fields for state selection by laser optical pumping.[1,9] The advantage of using this method is that lower-state intervals are measured directly. This increases the precision to which intervals can be measured by a factor of ~ 100 relative to the indirect optical measurements. The increased precision is essential to test *ab initio* theories.

In the present paper we report a completed study of the hyperfine structure (hfs) in the $3d^2$ configuration of Sc II. Our previous study of Sc II using only optical spectroscopy[10] allowed testing of *only* the magnetic-dipole hyperfine-interaction constants (A values) derived from multiconfiguration Dirac-Fock (MCDF) calculations. The electric-quadrupole constants (B values) were essentially untested because of large experimental uncertainties. Now, due to the increased precision of the double-resonance method, we are able to measure the B values well enough to test the MCDF theory[11] for the first time.

In Sec. II we describe the apparatus, the experimental procedure, and the observations. In Sec. III we present our analysis and results, and in Sec. IV we compare our results with the MCDF calculations.

II. EXPERIMENTAL APPARATUS AND TECHNIQUE

The apparatus has been described in detail elsewhere,[12–14] therefore the description given here is relatively brief except for those areas where improvements have been made to the apparatus and technique. A schematic diagram of the apparatus is shown in Fig. 1. A beam of metastable Sc ions was produced by an electron-impact ionization source, accelerated to 50 keV, mass analyzed, and collimated. Typical ion currents detected in a Faraday cup located after the probe region were 0.5–1 μA. The ion beam interacts collinearly with a frequency-stabilized cw dye laser (CR 699) over a total distance of 2.3 m. Our measurements required the use of four laser dyes: Rhodamine 6G, Rhodamine 110, and DCM were pumped with an argon-ion laser (Innova 100) in the visible mode while Stilbene 3 dye was pumped in the uv mode. We obtained 180 mW of tunable single-mode light at the peak of the Stilbene dye with 3 W of input uv power.

The optical measurements consist of exciting metasta-

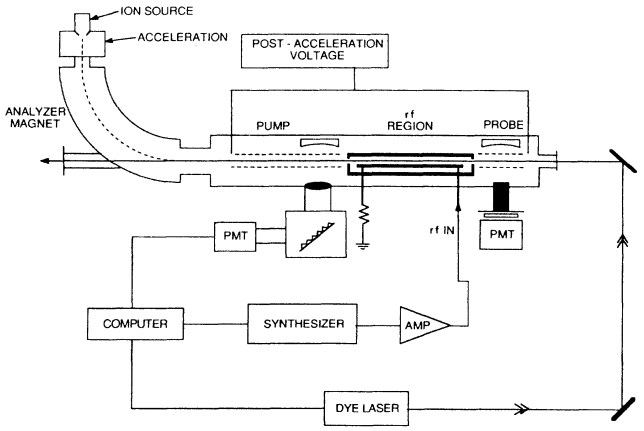

FIG. 1. Schematic diagram of the experimental apparatus used in the LIF and LRDR experiments. The pump region where optical pumping occurs, the rf region where repopulation takes place, and the probe region where fluorescence is detected are shown.

TABLE I. List of studied transitions in Sc II. The wavelengths of the transitions are listed in column 1, the upper and lower levels connected by the laser are listed in columns 2–5, and the interference filters used to isolate the decay channel are listed in column 6.

Laser wavelength (Å)	Config. *SLJ*	Even parity lower level (cm^{-1})	Config. *SLJ*	Odd parity upper level (cm^{-1})	Filter (Å)
4326.21	$3d^2\,^3F_2$	4802.75	$3d4p\,^3D_1^\circ$	27 917.69	3600
4306.92	$3d^2\,^3F_2$	4802.75	$3d4p\,^3D_2^\circ$	28 021.21	3600
4281.14	$3d^2\,^3F_2$	4802.75	$3d4p\,^3D_3^\circ$	28 161.03	3600
4321.93	$3d^2\,^3F_3$	4883.42	$3d4p\,^3D_2^\circ$	28 021.21	3600
4295.97	$3d^2\,^3F_3$	4883.42	$3d4p\,^3D_3^\circ$	28 161.03	3600
4315.29	$3d^2\,^3F_4$	4987.64	$3d4p\,^3D_3^\circ$	28 161.03	3600
4375.69	$3d^2\,^3F_4$	4987.64	$3d4p\,^3F_4^\circ$	27 841.17	3600
6606.43	$3d^2\,^1D_2$	10 944.56	$3d4p\,^1D_2^\circ$	26 081.32	4300
5676.87	$3d^2\,^3P_1$	12 101.50	$3d4p\,^3P_0^\circ$	29 736.22	3600
5657.90	$3d^2\,^3P_2$	12 154.42	$3d4p\,^3P_2^\circ$	29 823.93	3400
5684.21	$3d^2\,^3P_2$	12 154.42	$3d4p\,^3P_1^\circ$	29 742.16	3600
5526.80	$3d^2\,^1G_4$	14 261.32	$3d4p\,^1G_3^\circ$	32 349.98	3600

ble Sc ions from the $3d^2$ to the $3d4p$ configuration by absorption of a laser photon. The excitation is monitored by detecting the decay to the ground term in a photon-counting photomultiplier located in the probe region. The probe region is operated at small post-acceleration voltage (−100 V typically). This differential doppler shift is enough to confine the laser-induced fluorescence (LIF) to that region. In all of our spectra, the laser frequency was scanned with the ion energy fixed. The atomic lines used in this study are listed in Table I.

Experimentally we observe that the quality of the LIF spectra does not remain constant in time. A clean, fresh source and a well-overlapped ion-laser beam give the optical hyperfine spectrum shown in Fig. 2(a) [full width at half maximum (FWHM) of about 50 MHz]. However, a dirty source (insulators partially coated with conducting material from the charge after many days of use), and poor overlap produces a spectrum shown in Fig. 2(b)

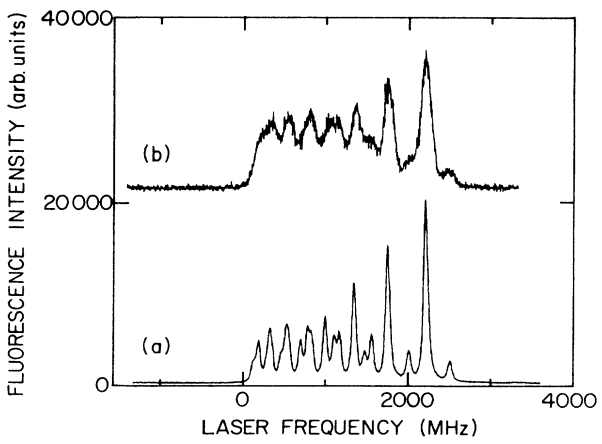

FIG. 2. The LIF spectrum shown in (a) was taken with a clean source and good overlap (see text). Most of the peaks are resolved, and the linewidth is ≃70 MHz. Spectrum (b) was taken with a dirty source and poor overlap. Most of the lines are not resolved and the linewidths ≃110 MHz. The optical transitions are between the $^3F_4$ and $^3F_4^\circ$ states.

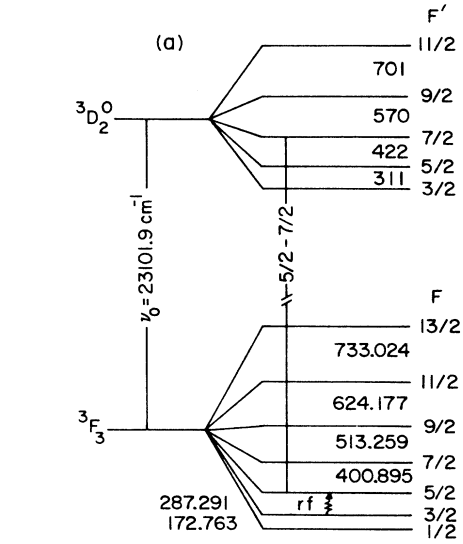

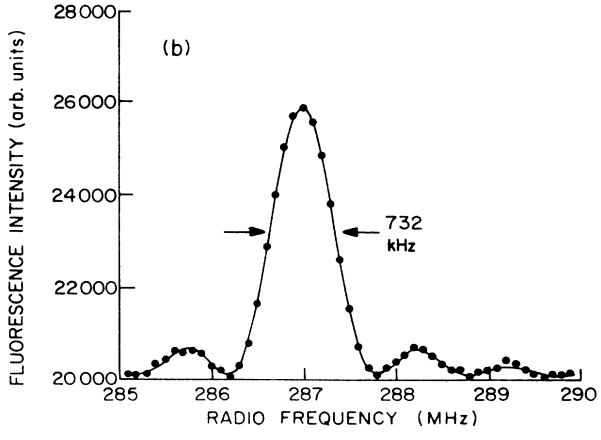

FIG. 3. The energy-level diagram of the hyperfine level of the $^3F_3$ and $^3D_2^\circ$ states is shown in (a). A laser-rf double-resonance spectrum for the transition $F_1=\frac{3}{2}\rightarrow F_2=\frac{5}{2}$ in the $^3F_3$ state is shown in (b). The solid line is a fit to a Rabi two-level model [Eq. (1)]. The linewidth obtained from the fit is 732 kHz, which is consistent with the ion transit time in the rf region of 1.08 μs at 50 keV energy.

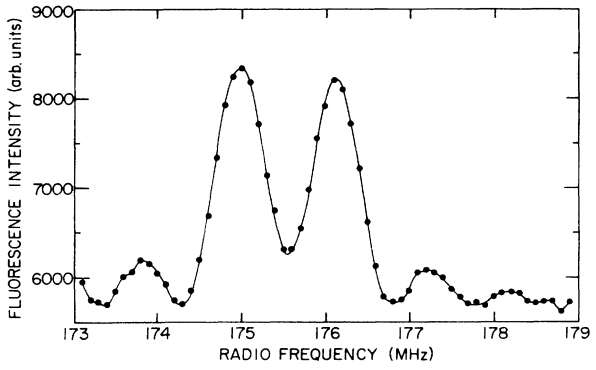

FIG. 4. The laser-rf double-resonance spectrum, for the transition $F=\frac{9}{2}\rightarrow\frac{7}{2}$ in the $^3F_4$ state, was taken with the ion-beam interacting with the rf field in the standing-wave configuration. This resulted in two peaks. The resonance frequency corresponds to the averaged position of the two peaks. The linewidth is ~700 kHz.

(FWHM of about 110 MHz). This linewidth results from transit-time broadening, lifetime broadening, and ion-source energy spread.

The LIF spectra are used to determine the magnitude and sign of the hfs parameters in both the upper and lower states. We have used previous results, along with new LIF spectra, to connect $3d^2\,^3F_{2,3,4}$ levels. Lower-level hfs parameters are then used as a starting point for high-resolution rf measurements.

The laser-rf double-resonance (LRDR) measurements require a population difference between adjacent hyperfine levels. This is achieved by introducing an upstream pump region (see Fig. 1), operated at the same post-acceleration voltage as the probe region, where a selected lower level is depleted by optical pumping. Typical depletions varied between 40–80 %. The ions then enter the magnetically shielded rf region,[13] where the laser is off resonance. Here the depleted level is repopulated by magnetic-dipole transitions of the type $F\leftrightarrow F\pm1$. The repopulation is detected as an increase in fluores-

TABLE II. The hyperfine intervals in Sc II from LRDR measurements are listed in column 3. Numbers in parentheses represent one standard deviation of the mean. The fitted hfs intervals listed in column 4 were evaluated using the A and B hfs parameters listed in Table III.

Level	Transition $F\rightarrow F+1$	Measured interval (MHz)	Fitted interval (MHz)	Residual measured-fitted interval (MHz)
$3d^2\,^3F_2$	$\frac{3}{2}\rightarrow\frac{5}{2}$	731.378(11)	731.378	0.0
	$\frac{5}{2}\rightarrow\frac{7}{2}$	1021.297(15)	1021.297	0.0
$3d^2\,^3F_3$	$\frac{1}{2}\rightarrow\frac{3}{2}$	172.763(13)	172.764	−0.001
	$\frac{3}{2}\rightarrow\frac{5}{2}$	287.340(20)	287.339	0.001
	$\frac{11}{2}\rightarrow\frac{13}{2}$	733.024(25)	733.024	0.000
$3d^2\,^3F_4$	$\frac{3}{2}\rightarrow\frac{5}{2}$	98.938(20)	98.936	0.002
	$\frac{5}{2}\rightarrow\frac{7}{2}$	137.634(19)	137.628	0.006
	$\frac{7}{2}\rightarrow\frac{9}{2}$	175.428(20)	175.440	−0.012
	$\frac{9}{2}\rightarrow\frac{11}{2}$	212.119(10)	212.117	0.002
	$\frac{11}{2}\rightarrow\frac{13}{2}$	247.411(30)	247.410	0.001
$3d^2\,^1D_2$	$\frac{3}{2}\rightarrow\frac{5}{2}$	369.920(12)	369.911	0.009
	$\frac{5}{2}\rightarrow\frac{7}{2}$	519.820(12)	519.830	−0.010
	$\frac{7}{2}\rightarrow\frac{9}{2}$	671.705(10)	671.704	0.001
$3d^2\,^3P_1$	$\frac{5}{2}\rightarrow\frac{7}{2}$	360.881(10)	360.881	0.0
	$\frac{7}{2}\rightarrow\frac{9}{2}$	495.610(14)	495.610	0.0
$3d^2\,^3P_2$	$\frac{3}{2}\rightarrow\frac{5}{2}$	79.235(19)	79.208	0.027
	$\frac{5}{2}\rightarrow\frac{7}{2}$	105.349(25)	105.361	−0.012
	$\frac{7}{2}\rightarrow\frac{9}{2}$	125.960(20)	125.980	−0.020
	$\frac{9}{2}\rightarrow\frac{11}{2}$	139.497(14)	139.488	0.009
$3d^2\,^1G_4$	$\frac{5}{2}\rightarrow\frac{7}{2}$	486.330(10)	486.339	−0.009
	$\frac{7}{2}\rightarrow\frac{9}{2}$	619.473(10)	619.476	0.006
	$\frac{9}{2}\rightarrow\frac{11}{2}$	748.232(10)	748.226	0.006
	$\frac{11}{2}\rightarrow\frac{13}{2}$	871.640(10)	871.644	−0.004

cence in the probe region. A LRDR spectrum is accumulated by recording the fluorescence intensity in the probe region as a function of the applied frequency in the rf region. A typical spectrum and the LRDR principle are illustrated in Fig. 3.

An important experimental feature which improved both the LIF and LRDR spectra was the implementation of an active correction to the post-acceleration voltage which compensated for long term (>0.1 s) fluctuations in the platform voltage. The correction voltage was derived through a differential voltmeter in combination with a operational amplifier. With the correction voltage applied, both the quality of the data and the efficiency in acquisition were substantially improved.

III. ANALYSIS AND RESULTS

The rf resonances were fitted to a Rabi two-level model[15] in order to extract the line center from the data. The rf transition probability $P(t,\omega_0)$ is given by

$$P(t,\omega_0)=\frac{A(2b)^2}{(\omega_0-\omega)^2+(2b)^2}\times\sin^2\left[\frac{t}{2}[(\omega_0-\omega)^2+(2b)^2]^{1/2}\right],$$

where ω_0 is the line center, A is the amplitude, t is the transit time, and $2b$ is the strength of the transition.

In the actual fitting procedure used, the Rabi function was normalized to unity at $\omega=\omega_0$ to produce a realistic amplitude A and a linear background was introduced. In fitting the rf spectra, the time parameter was often varied to compare with the known transit time. This was useful, in cases where the statistics were poor, as a check on the fitting procedure. Parameters t and b are highly correlated in fitting but the parameter of most interest, ω_0, is independent of how the data is fitted. Typical linewidths (FWHM) were found to be 700–800 kHz with a typical χ^2 per degree of freedom of 1.7. The errors quoted in the tables are the standard deviations of the measurements.

For each rf transition, we derived the resonance frequency for data taken with the rf field copropagating and counterpropagating with the ion beam and applied a correction for the doppler shift in each case. Measurements were also taken in the standing-wave configuration (Fig. 4). The arithmetic averages of these measurements were taken and are shown in Table II.

The relevance of light shifts[16] to each measured rf interval was estimated by calculating the effect from known power densities, detuning, transition probabilities,[17] and assuming optimum laser-beam–ion-beam overlap in the rf region. These calculations revealed those levels for which the light shift was a serious problem. A comparison with experimental data in the $^3P_1$ state for various laser powers showed the calculations, in our case, to be an overestimate but a good guide nevertheless. In the case of $^3F_3$ only three intervals survive the criterion of having calculated light shifts less than the data scatter. For $^3P_2$ levels it was necessary to change the pump- and probe-region voltages to 400 V, corresponding to detunings of 3200 MHz, in order to satisfy the same criterion. In all cases, only data for which the light shift is small in comparison with data scatter, was used in the determination of the hyperfine constants.

Using the standard formula given by Schwartz[18] the magnetic dipole A, and the electric quadrupole hfs constants B, were determined using the hfs splittings listed in Table II. In all cases listed, the octupole coupling constant was much too small to be measured with this level of precision. The hfs parameters are listed in Table III.

TABLE III. List of hyperfine A and B. Numbers in parentheses represent one standard deviation.

Level (cm^{-1})	Config.	SLJ	A (MHz)	B (MHz)
4802.75	$3d^2$	$^3F_2$	290.669(12)[a]	−10.540(83)[a]
4883.42	$3d^2$	$^3F_3$	113.674(3)[a]	−12.615(40)[a]
4957.64	$3d^2$	$^3F_4$	38.357(2)[a]	−16.456(75)[a]
10 944.56	$3d^2$	$^1D_2$	149.361(2)[a]	7.818(30)[a]
12 101.50	$3d^2$	$^3P_1$	−107.501(2)[a]	−12.297(6)[a]
12 154.42	$3d^2$	$^3P_2$	−27.732(2)[a]	22.127(23)[a]
14 261.32	$3d^2$	$^1G_4$	135.232(1)[a]	−63.439(40)[a]
26 081.34	$3d4p$	$^1D_2^\circ$	215.7(8)[b]	18.0(7)[b]
27 443.71	$3d4p$	$^3F_2^\circ$	366.8(1)[b]	−40.0(14)[b]
27 602.45	$3d4p$	$^3F_3^\circ$	205.4(6)[b]	−70.0(18)[b]
27 841.17	$3d4p$	$^3F_4^\circ$	102.3(1)[c]	−84.0(2)[c]
27 917.69	$3d4p$	$^3D_1^\circ$	304.7(2)[c]	4.5(8)[c]
28 021.21	$3d4p$	$^3D_2^\circ$	125.3(1)[c]	10.0(1)[c]
28 161.03	$3d4p$	$^3D_3^\circ$	99.5(1)[c]	21.0(2)[c]
29 742.16	$3d4p$	$^3P_1^\circ$	255.0(2)[b]	10.0(8)[b]
29 823.03	$3d4p$	$^3P_2^\circ$	106.2(1)[c]	20.0(1)[c]
32 349.98	$3d4p$	$^1F_3^\circ$	191.1(3)[c]	−82.0(4)[c]

[a]Derived from LRDR measurements.
[b]From optical measurements (Ref. 10) only.
[c]From combination of LRDR measurements for the lowest state with optical spectra (as described in text).

TABLE IV. Comparison of the A and B values derived from LRDR measurements with *ab initio* MCDF values. MCDF values are calculated using $I=\frac{7}{2}$, $\mu_I=4.74875$ nm, and $Q=-0.22$ b from Ref. 22.

Config. *SLF*	A(obs) (MHz)	A(MCDF) (MHz)	ΔA	B(obs) (MHz)	B(MCDF) (MHz)	ΔB
$3d^2\,^3F_2$	290.669	221.2	69.5	−10.54	−11.8	1.3
$3d^2\,^3F_3$	113.674	144.6	−30.9	−12.62	−12.9	0.3
$3d^2\,^3F_4$	38.357	108.3	−69.9	−16.46	−17.3	0.8
$3d^2\,^1D_2$	149.361	146.6	2.8	7.82	14.3	−6.5
$3d^2\,^3P_1$	−107.501	−1.8	−105.7	−12.30	−11.6	−0.7
$3d^2\,^3P_2$	−27.732	85.9	−113.6	22.13	23.2	−1.1
$3d^2\,^1G_4$	135.232	143.2	−7.9	−63.44	−65.4	2.0

A comparison of these results with previous measurements[10,19] shows a 150-fold increase in precision. Using these constants, the hyperfine intervals were evaluated and listed in Table II, along with the measured ones. The size of the residuals is indicative of internal consistency for most levels.

Nearby fine-structure states can perturb the energy levels within a hyperfine multiplet through off-diagonal hfs interactions. The magnitude of the perturbations can be estimated through second-order perturbation theory:

$$\delta E_{\rm hfs}(\alpha SLJIFM)=\sum_{J'}\frac{|\langle\alpha SLJIFM|H_{\rm hfs}|\alpha SLJ'IFM\rangle|^2}{E(\alpha SLJ)-E(\alpha SLJ')}.$$

The appropriate matrix elements for the l^N configuration for the $M-1$ and $E-2$ interactions are found in Ref. 20. The required radial integrals a_{3d}^{10}, a_{3d}^{12}, a_{3d}^{01}, and b_d are derived from effective-operator fitting of the A and B values of all levels within the $3d^2$ configuration listed in Table III. The values of the radial parameters are $a_{3d}^{10}=a_{3d}^{12}=143.3$ MHz, $a_{3d}^{10}\equiv C'=-229.6$ MHz, and $b_{3d}=-55.0$ MHz.

Using these values, second-order energy shifts were evaluated. Only perturbations from members of the same fine-structure multiplet were found to be significant. In the most severe case ($3d^2\,^3P_1$), the off-diagonal hfs interactions shift levels by ~600 kHz and intervals by ~1.2 MHz. This results in a change of less than 70 kHz (0.1%) in the A value and of less than 1 MHz (8%) in the B value. Since the residuals before and after making the second-order corrections are roughly equivalent (and reasonable in view of the scatter in the data) and the change in the derived A and B values is relatively small, we have decided to use the intervals listed in Table II (i.e., the measured intervals) and the corresponding A's and B's (Table III) for further discussion.

The hfs constants of the upper states were also determined and are shown in Table III. To extract these values we used the optical spectra in conjunction with the hfs constants of the lower state (determined with rf precision). Again, a comparison of these results with our previous measurements, shows an improvement by a factor of 5. The main factor in this improvement was the voltage correction system which yielded more accurate optical spectra.

IV. COMPARISON OF LRDR RESULTS WITH THEORY

Previously we discussed hfs in the $3d^2$ and $3d4p$ configurations in terms of the effective-operator method of Sandars and Beck and *ab initio* MCDF calculations. While the simple optical LIF measurements were sufficient to test the MCDF calculations of the A values, a meaningful comparison with theory for the B values was not possible due to the large experimental uncertainties. The new experimental results presented in Sec. III now permit this comparison to be made. In this section we summarize the previous findings regarding the deficiencies of the MCDF theory in evaluating the A values, present the new calculations for the $^3F_{2,3,4}$ levels and compare the LRDR B values with theoretical predictions.

The experimental and MCDF calculated A values for the states in the $3d^2$ configuration were compared previously. It was found that while the MCDF predicted A values agreed well for singlet states (within 6%), predictions for triplet states were very poor (greater than 400% error for $3d^2\,^3P_2$). The Sandars-Beck effective-operator treatment showed that the magnetic-dipole hfs is actually dominated by the contact contribution of the $3d$ electron. It was argued that the source of the contact contribution was polarization of the [Ar] core in the triplet states and that the neglect of the core polarization was the cause of the discrepancy between experiment and theory. The new results on the $^3F_{2,3,4}$ states corroborate the earlier findings (see Table IV).

The experimental and MCDF calculated B values are also shown in Table IV. Unlike the A values, generally good agreement is found between theory and experiment, with the sole exception of the $3d^2\,^1D_2$ state. The better agreement is, in general, to be expected.[21] Configuration interaction effects are represented by a simple scaling, $B_{\rm true}=1/(1-R_{nl})B_{\rm obs}$, where R_{nl} is the Sternheimer shielding factor. The core polarization (a form of configuration interaction) which dominates the dipole hfs of the triplet states has no effect on the B values since $ns\rightarrow ns$ excitations play no role in the electric quadrupole interaction. Since distortion of the electron core by the nuclear-quadrupole moment (Sternheimer effect) is not accounted for in the MCDF calculations, the good agreement between experiment and theory indicates that quad-

rupole shielding, R_{3d}, is quite small. The reason for the disagreement between experiment and theory for the $3d^2\,{}^1D_2$ state is still unknown.

V. CONCLUSIONS

We have carried out laser-rf double-resonance measurements on Sc II with an upgraded ion-beam apparatus. The hyperfine structure of all levels in the metastable $3d^2$ configuration has been measured with rf precision, improving the previous measurements by more than a factor of 150 for the A values and by more than a factor of 300 for the B values. The hyperfine constants of the $3d4p$ configuration have also been improved by at least a factor of 5 for both the A and B values.

The improved B values have allowed, for the first time, a meaningful comparison to be made with the MCDF calculated values. The comparison showed that, unlike the A values, the electric-quadrupole hyperfine-interaction constants were well predicted (to within $\sim$ 10%) by the MCDF calculations. Configuration-interaction effects on the B values, which would appear in Sternheimer shielding factors, were small. This contrasts markedly with the situation of the A values, where core-polarization effects, which are unaccounted for in the MCDF theory, dominate.

ACKNOWLEDGMENTS

We would like to thank W. J. Childs and H. G. Berry for helpful discussions and suggestions during this work. We would also like to thank C. Kurtz and M. L. A. Raphaelian for their assistance during the upgrade of the apparatus and M. J. Marjanovic for programming assistance. The research was supported by the U. S. Department of Energy, Office of Basic Energy Sciences, under Contract No. W-31-109-ENG-38.

*Also at University of Chicago, Chicago, IL 60637.

[1]S. D. Rosner, R. A. Holt, and T. D. Gaily, Phys. Rev. Lett. **35**, 785 (1975); W. Ertmer and B. Hofer, Z. Phys. A **276**, 9 (1976).

[2]T. J. Scholl, T. D. Gaily, R. A. Holt, and S. D. Rosner, Phys. Rev. A. **33**, 2396 (1986).

[3]H. Dehmelt, *Advances in Laser Spectroscopy*, Vol. 95 of *NATO ASI Series B: Physics* (Plenum, New York, 1983), p. 153.

[4]R. Trainham, R. M. Jopson, and D. J. Larson, Phys. Rev. A **39**, 3223 (1989).

[5]R. Novick and E. D. Commins, Phys. Rev. **111**, 822 (1958).

[6]S. D. Rosner, T. D. Gaily, and R. A. Holt, Phys. Rev. Lett. **40**, 851 (1978).

[7]A. Sen and W. J. Childs, Phys. Rev. A **36**, 1983 (1987).

[8]I. I. Rabi, J. R. Zacharias, S. Millman, and P. Kusch, Phys. Rev. **53**, 318 (1938); J. R. Zacharias, *ibid.* **61**, 270 (1942).

[9]J. Brossel, A. Kastler, and J. Winter, J. Phys. Radium **13**, 668 (1952).

[10]L. Young, W. J. Childs, T. Dinneen, C. Kurtz, H. G. Berry, L. Engstrom, and K. T. Cheng, Phys. Rev. A **37**, 4213 (1988).

[11]K. T. Cheng and W. J. Childs, Phys. Rev. A **31**, 2775 (1985).

[12]L. Young, W. J. Childs, H. G. Berry, C. Kurtz, and T. Dinneen, Phys. Rev. A **36**, 2148 (1987).

[13]A. Sen, L. S. Goodman, and W. J. Childs, Rev. Sci. Instrum. **59**, 74 (1988).

[14]L. Young, T. Dinneen, and N. B. Mansour, Phys. Rev. A **38**, 3812 (1988).

[15]N. F. Ramsey, *Molecular Beams* (Clarendon, Oxford, 1956), Chap. V.

[16]G. Borghs, P. DeBisschop, J. Odeurs, R. E. Silverans, and M. Van Hove, Phys. Rev. A **31**, 1434 (1985).

[17]*Experimental Transition Probabilities for Spectral Lines of Seventy Elements*, Natl. Bur. Stand. Monograph No. 53, edited by C. H. Corliss and W. R. Bozman (U.S. GPO, Washington, D.C., 1962).

[18]C. Schwartz, Phys. Rev. **97**, 380 (1955).

[19]A. Arnesen *et al.*, Astron. Astrophys. **106**, 327 (1982).

[20]W. J. Childs, Case Stud. Atom. Phys. **3**, 215 (1973).

[21]B. G. Wybourne, *Spectroscopic Properties of Rare Earths* (Wiley, New York, 1965), pp. 148–153.

[22]G. H. Fuller, J. Phys. Chem. Ref. Data **5**, 835 (1976).